arXiv:1805.06773v1 [math.OC] 15 May 2018

R2-based hypervolume contribution approximation in multi-objective optimization

Ke Shang[1,2], Hisao Ishibuchi[1], Xizi Ni[1], and Min-Ling Zhang[2]

[1] Department of Computer Science and Engineering,
Southern University of Science and Technology, Shenzhen, China
kshang@foxmail.com, hisao@sustc.edu.cn
[2] School of Computer Science and Engineering,
Southeast University, Nanjing, China

Abstract. In this paper, a new hypervolume contribution approximation method is proposed which is formulated as an R2 indicator. The basic idea of the proposed method is to use different line segments only in the hypervolume contribution region for the hypervolume contribution approximation. Compared with the traditional method which is based on the R2 contribution to approximate the hypervolume contribution, the new method can directly approximate the hypervolume contribution and will utilize all the direction vectors only in the hypervolume contribution region. The new method, the traditional method and a simple method are compared through numerical experiments. Our experimental results show the overwhelming superiority of the new method over the other two methods, where the new method achieves the best performances for comparing hypervolume contributions of different solutions and identifying the solution with the smallest hypervolume contribution.

Keywords: Hypervolume contribution, R2 indicator, Multi-objective optimization

1 Introduction

Hypervolume [15] is a widely used performance indicator in the Evolutionary Multi-objective Optimization (EMO) community due to its well-known unique property (i.e., Pareto compliance) among all the existing indicators. The bottleneck of the hypervolume applicability in Evolutionary Multi-objective Optimization Algorithms (EMOA) is the increasing computational burden as the dimentionality of the objective space increases. Efforts in the hypervolume approximation [2,6] have been done to increase the applicability of the hypervolume to high-dimensional spaces, including the Monte Carlo hit-or-miss method [1,2] and the achievement scalarizing function method [6,7].

In the achievement scalarizing function method, the hypervolume is approximated by a number of achievement scalarizing functions with uniformly distributed weight vectors. Each achievement scalarizing function with a different weight vector is used to measure the distance from the reference point to the

attainment surface of the solution set. Then the average distance from the reference point to the attainment surface over a large number of weight vectors is calculated as the hypervolume approximation.

The achievement scalarizing function method can be formularized in the form of an R2 indicator. In [10], an R2 indicator is proposed based on a new Tchebycheff function which is called 2-Tch. The proposed R2 indicator shows a clear geometric property to indirectly approximate the hypervolume, which is a formularization of the achievement scalarizing function method. In [12], a new R2 indicator is proposed based on the Divergence theorem and Riemann sum approximation for better hypervolume approximation. The new R2 indicator significantly improved the approximation quality for the hypervolume compared with the achievement scalarizing function method.

In the hypervolume-based EMOA (e.g., SMS-EMOA [3]), the hypervolume contribution is used to evaluate the fitness value of each individual. With a steady-state $(\mu+1)$ES-type generation update mechanism, the worst individual with the smallest hypervolume contribution is eliminated from the population. Thus, the hypervolume contribution plays an important role in the hypervolume-based EMOA. This paper investigates hypervolume contribution approximation methods based on the R2 indicator. The main contribution of this paper is that a new method which is formularized as an R2 indicator is proposed for the hypervolume contribution approximation. Compared with the traditional method which approximates the hypervolume contribution by the R2 contribution, the new method can directly approximate the hypervolume contribution and is able to achieve a high approximation quality with only a small number of direction vectors.

The remainder of the paper is organized as follows. Section 2 gives the preliminaries of the paper. R2-based hypervolume contribution approximation methods are investigated in Section 3. Numerical studies are given in Section 4, and we conclude the paper in Section 5.

2 Preliminaries

2.1 Hypervolume and hypervolume contribution

Given a reference point $\mathbf{r}$ and an approximation solution set A, the hypervolume of the set A is defined as:

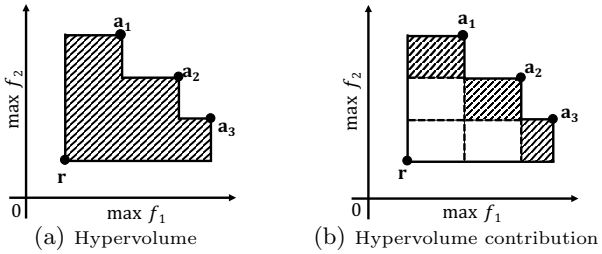
$$HV(A,\mathbf{r}) = \mathcal{L}\left(\bigcup_{\mathbf{a}\in A}\{\mathbf{b}|\mathbf{a}\succ\mathbf{b}\succ\mathbf{r}\}\right) \tag{1}$$

where $\mathcal{L}(.)$ is the Lebesgue measure of a set, and $\mathbf{a}\succ\mathbf{b}$ means $\mathbf{a}$ dominates $\mathbf{b}$.

For a solution $\mathbf{s}\in A$, its hypervolume contribution is defined as:

$$C_{HV}(\mathbf{s},A,\mathbf{r}) = HV(A,\mathbf{r}) - HV(A\setminus\{\mathbf{s}\},\mathbf{r}) \tag{2}$$

Fig. 1 gives an illustration of the hypervolume and hypervolume contribution. The hypervolume is the shaded area of the enclosed polygon in Fig. 1 (a). The



(a) Hypervolume (b) Hypervolume contribution

Fig. 1. An illustration of the hypervolume and the hypervolume contribution

hypervolume contribution of each solution is the shaded area which is uniquely dominated by the corresponding solution in Fig. 1 (b).

2.2 R2 indicator for hypervolume approximation

Given a solution set A, a set of direction vectors Λ, and a utopian point $\mathbf{r}^*$, the R2 indicator based on the 2-Tch function [10] is defined as:

$$R_2^{2tch}(A, \Lambda, \mathbf{r}^*) = \frac{1}{|\Lambda|} \sum_{\lambda \in \Lambda} \min_{\mathbf{a} \in A} \left\{ g^{2tch}(\mathbf{a}|\lambda, \mathbf{r}^*) \right\} \tag{3}$$

where the 2-Tch function is defined as follows:

$$g^{2tch}(\mathbf{a}|\lambda, \mathbf{r}^*) = \max_{j \in \{1,\ldots,m\}} \left\{ \frac{|r_j^* - a_j|}{\lambda_j} \right\} \tag{4}$$

In Eq. (4), $\lambda = (\lambda_1, \lambda_2, ..., \lambda_m)$ is a given direction vector with $\|\lambda\|_2 = 1$ and $\lambda_i \geq 0$, $i = 1, ..., m$.

Fig. 2 (a) shows the geometric property of R_2^{2tch}. In this figure, $\mathbf{r}^*$ is the utopian point and $\mathbf{r}$ is the reference point for the hypervolume calculation. Suppose a line follows the direction λ and passes through $\mathbf{r}^*$ and intersects with the attainment surface of the solution set A at $\mathbf{p}$, then the length of the line segment with the end points $\mathbf{r}^*$ and $\mathbf{p}$ is determined by $\min_{\mathbf{a} \in A} \left\{ g^{2tch}(\mathbf{a}|\lambda, \mathbf{r}^*) \right\}$, and R_2^{2tch} is the average length of the line segments with different directions as shown in Fig. 2 (a).

The idea of using different line segments starting from a reference point to the attainment surface of the solution sets for the hypervolume approximation was firstly proposed in [6]. Intuitively, the average length of the line segments in Fig. 2 (b) is closely related to the hypervolume.

The R_2^{2tch} indicator cannot be directly used for the hypervolume approximation as shown in Fig. 2 (a). Its modified version which is able to directly approximate the hypervolume is defined as follows:

$$R_2^{mtch}(A, \Lambda, \mathbf{r}) = \frac{1}{|\Lambda|} \sum_{\lambda \in \Lambda} \max_{\mathbf{a} \in A} \left\{ g^{mtch}(\mathbf{a}|\lambda, \mathbf{r}) \right\} \tag{5}$$

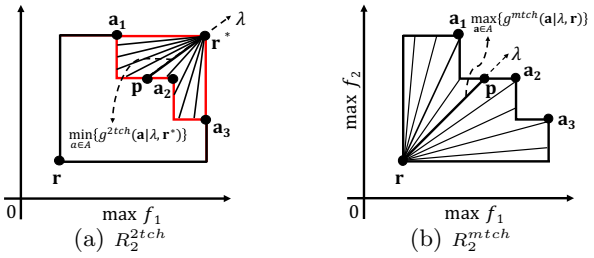


Fig. 2. An illustration of the geometric property of R_2^{2tch} and R_2^{mtch}.

where g^{mtch} function is defined as follows:

$$g^{mtch}(\mathbf{a}|\lambda, \mathbf{r}) = \min_{j\in\{1,\ldots,m\}} \left\{ \frac{|r_j - a_j|}{\lambda_j} \right\} \tag{6}$$

where $\mathbf{r}$ is the reference point for the hypervolume calculation, λ is a given direction vector which is the same as in g^{2tch} in Eq. (4).

It is easy to examine that the R_2^{mtch} indicator has a geometric property as shown in Fig. 2 (b), which can be used directly for the hypervolume approximation.

In our previous work [12], a new R2 indicator is proposed for better hypervolume approximation. The new R2 indicator is derived based on the Divergence theorem and Riemann sum approximation. It is defined as follows:

$$R_2^{HV}(A, \Lambda, \mathbf{r}) = \frac{1}{|\Lambda|} \sum_{\lambda\in\Lambda} \max_{\mathbf{a}\in A} \left\{ g^{mtch}(\mathbf{a}|\lambda, \mathbf{r}) \right\}^m \tag{7}$$

Comparing Eq. (7) with Eq. (5), we can see that the only difference between R_2^{mtch} and R_2^{HV} is the added exponential m in R_2^{HV}. This small change in R_2^{HV} significantly improves the approximation quality of the R2 indicator for the hypervolume. For detailed explanations of the new R2 indicator, please refer to our previous work [12].

3 R2-based hypervolume contribution approximation

3.1 Traditional method and its drawbacks

As shown in the previous section, the R2 indicator (e.g., R_2^{mtch} and R_2^{HV}) can be used to approximate the hypervolume. We can also use the R2 indicator to approximate the hypervolume contribution. The simplest and straightforward method is to use the R2 contribution to approximate the hypervolume contribution.

For a solution $\mathbf{s} \in A$, its R2 contribution is defined as follows:

$$C_{R_2}(\mathbf{s}, A, \Lambda, \mathbf{r}) = R_2(A, \Lambda, \mathbf{r}) - R_2(A \setminus \{\mathbf{s}\}, \Lambda, \mathbf{r}) \tag{8}$$

where R_2 can be R_2^{mtch} and R_2^{HV} for the hypervolume approximation.

According to the definition of the R2 contribution, the traditional method for the hypervolume contribution approximation (as illustrated in Fig. 3) can be described by the following three steps:

- Step 1: Calculate the R2 value of the solution set A.
- Step 2: Calculate the R2 value of the solution set $A \setminus \{\mathbf{s}\}$.
- Step 3: Calculate the difference between the above two R2 values as the hypervolume contribution approximation of the solution $\mathbf{s}$.

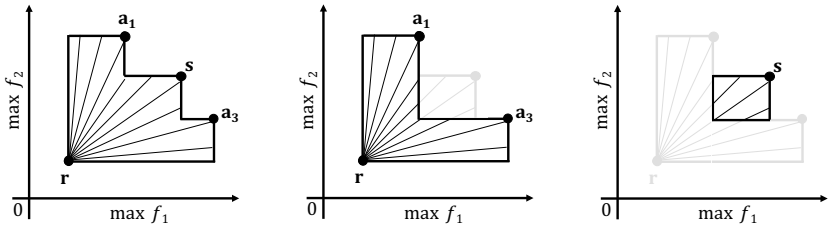


Fig. 3. An illustration of the traditional method for the hypervolume contribution approximation. The hypervolume contribution of solution $\mathbf{s}$ is approximated by the difference between the R2 values of the solution sets $\{\mathbf{a}_1, \mathbf{s}, \mathbf{a}_3\}$ and $\{\mathbf{a}_1, \mathbf{a}_3\}$.

The drawbacks of the traditional method are summarized as follows:

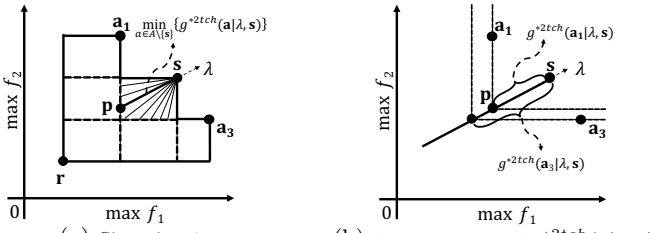
1. In order to obtain the hypervolume contribution approximation of a solution, we need to calculate R2 values for two solution sets. The hypervolume contribution cannot be approximated directly.
2. Usually there exist errors in the R2 approximation for the hypervolume. So the error of the hypervolume contribution approximation could be amplified by the errors of the two R2 values. For this reason, the approximation accuracy of the traditional method may be low.
3. In order to improve the approximation accuracy, a large number of vectors are needed for calculating the R2 indicator. Thus, the amount of computation in the traditional method could be large so as to achieve a high approximation accuracy.

3.2 A new method for hypervolume contribution approximation

In this subsection, a new method is proposed for the hypervolume contribution approximation. The basic idea is to use different line segments only in the hypervolume contribution region for the hypervolume contribution approximation.

The proposed idea is illustrated in Fig. 4 (a). In Fig. 4 (a), the hypervolume contribution region of solution $\mathbf{s}$ is occupied by the line segments with different

directions which start from solution $\mathbf{s}$ and end on the boundaries of the hypervolume contribution region of solution $\mathbf{s}$. Then we can utilize all the line segments in the hypervolume contribution region to approximate the corresponding hypervolume contribution, which is similar to R_2^{mtch} or R_2^{HV} for the hypervolume approximation.



(a) Situation 1 (b) Contour lines of $g^{*2tch}(\mathbf{a}|\lambda, \mathbf{s})$

Fig. 4. An illustration of the proposed idea (Situation 1).

First, let us consider the situation in Fig. 4 (a). In this situation, the line segments in the hypervolume contribution region of the solution $\mathbf{s}$ only intersect with the attainment surface of the solution set $A \setminus \{\mathbf{s}\}$, i.e., the lengths of the line segments are only determined by the solution set $A \setminus \{\mathbf{s}\}$. This situation is similar to R_2^{2tch} as illustrated in Fig. 2 (a).

Given a direction vector λ, a solution $\mathbf{s}$ and a solution set $A \setminus \{\mathbf{s}\}$, the length of the line segment in Fig. 4 (a) can be calculated by the following formula:

$$L(\mathbf{s}, A, \lambda) = \min_{\mathbf{a} \in A \setminus \{\mathbf{s}\}} \left\{ g^{*2tch}(\mathbf{a}|\lambda, \mathbf{s}) \right\} \tag{9}$$

where the $g^{*2tch}(\mathbf{a}|\lambda, \mathbf{s})$ function is defined as follows:

$$g^{*2tch}(\mathbf{a}|\lambda, \mathbf{s}) = \begin{cases} \max_{j \in \{1,\ldots,m\}} \left\{ \frac{s_j - a_j}{\lambda_j} \right\}, & \text{maximization case} \\ \max_{j \in \{1,\ldots,m\}} \left\{ \frac{a_j - s_j}{\lambda_j} \right\}, & \text{minimization case} \end{cases} \tag{10}$$

In the maximization case which is considered in Fig. 4 (a), notice that $g^{*2tch}(\mathbf{a}|\lambda, \mathbf{s})$ is slightly different from $g^{2tch}(\mathbf{a}|\lambda, \mathbf{r}^*)$ in Eq. (4) that there is no absolute value sign in $g^{*2tch}(\mathbf{a}|\lambda, \mathbf{s})$ in Eq. (10). The reason can be clearly explained by Fig. 4 (b), which shows the contour lines of $g^{*2tch}(\mathbf{a}|\lambda, \mathbf{s})$ in the maximization case. If the absolute value sign is added in $g^{*2tch}(\mathbf{a}|\lambda, \mathbf{s})$, then the contour line property will be changed and the lengths of the line segments may not be correctly calculated. The same analysis can be applied to $g^{*2tch}(\mathbf{a}|\lambda, \mathbf{s})$ in the minimization case.

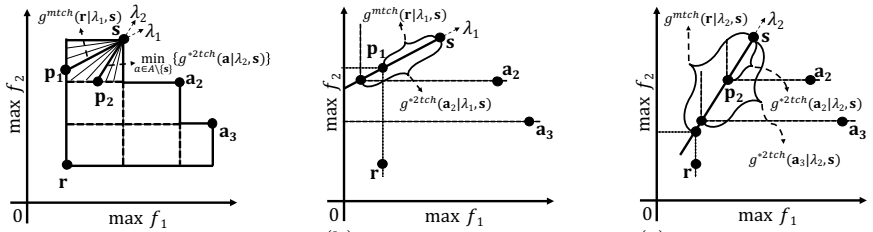
Next, let us consider the situation in Fig. 5 (a). In this situation, the line segments in the hypervolume contribution region of the solution $\mathbf{s}$ not only intersect with the attainment surface of the solution set $A \setminus \{\mathbf{s}\}$ but also intersect with the

hypervolume boundary of the solution set A associated with the reference point $\mathbf{r}$. For the line segments intersecting with the attainment surface of the solution set $A \setminus \{\mathbf{s}\}$, the lengths can be calculated by Eq. (9). While for the line segments intersecting with the hypervolume boundary associated with the reference point $\mathbf{r}$, the lengths are calculated as follows:

$$L(\mathbf{s}, \mathbf{r}, \lambda) = g^{mtch}(\mathbf{r}|\lambda, \mathbf{s}) \tag{11}$$

where $g^{mtch}(\mathbf{r}|\lambda, \mathbf{s})$ is defined as:

$$g^{mtch}(\mathbf{r}|\lambda, \mathbf{s}) = \min_{j \in \{1,\ldots,m\}} \left\{ \frac{|s_j - r_j|}{\lambda_j} \right\} \tag{12}$$



(a) Situation 2 (b) Contour lines for λ_1 (c) Contour lines for λ_2

Fig. 5. An illustration of the proposed idea (Situation 2).

Notice that $g^{mtch}(\mathbf{r}|\lambda, \mathbf{s})$ in Eq. (12) and $g^{mtch}(\mathbf{a}|\lambda, \mathbf{r})$ in Eq. (6) are in the same form. Fig. 5 (b) and (c) show the contour lines of $g^{mtch}(\mathbf{r}|\lambda, \mathbf{s})$ and $g^{*2tch}(\mathbf{a}|\lambda, \mathbf{s})$ for λ_1 and λ_2 respectively. From Fig. 5 (b) for a line segment intersecting with the hypervolume boundary associated with the reference point $\mathbf{r}$, its length is $L(\mathbf{s}, \mathbf{r}, \lambda_1)$ and $L(\mathbf{s}, \mathbf{r}, \lambda_1) < L(\mathbf{s}, A, \lambda_1)$ holds. From Fig. 5 (c) for a line segment intersecting with the attainment surface of the solution set $A \setminus \{\mathbf{s}\}$, its length is $L(\mathbf{s}, A, \lambda_2)$ and $L(\mathbf{s}, A, \lambda_2) < L(\mathbf{s}, \mathbf{r}, \lambda_2)$ holds.

Wrapping up the above two situations, the length of any line segment along direction λ starting from $\mathbf{s}$ and intersecting with the boundaries of the hypervolume contribution region is calculated as follows:

$$L(\mathbf{s}, A, \mathbf{r}, \lambda) = \min\{L(\mathbf{s}, A, \lambda), L(\mathbf{s}, \mathbf{r}, \lambda)\} \tag{13}$$

Based on the lengths of the line segments in the hypervolume contribution region, we can define the following R2 indicator to approximate the hypervolume contribution:

$$\begin{aligned} R_2^{HVC}(\mathbf{s}, A, \Lambda, \mathbf{r}) &= \frac{1}{|\Lambda|} \sum_{\lambda \in \Lambda} L(\mathbf{s}, A, \mathbf{r}, \lambda)^\alpha \\ &= \frac{1}{|\Lambda|} \sum_{\lambda \in \Lambda} \min \left\{ \min_{\mathbf{a} \in A \setminus \{\mathbf{s}\}} \left\{ g^{*2tch}(\mathbf{a}|\lambda, \mathbf{s}) \right\}, g^{mtch}(\mathbf{r}|\lambda, \mathbf{s}) \right\}^\alpha \end{aligned} \tag{14}$$

where $\alpha = 1$ if we want to use the average length of the line segments for the approximation, or $\alpha = m$ if we want to use the average m powered length of the line segments for the approximation.

Compared with the traditional method described in the previous subsection, the proposed new method for the hypervolume contribution approximation has the following advantages:

1. The hypervolume contribution approximation of a solution can be directly calculated by Eq. (14).
2. The new method will utilize all direction vectors only in the hypervolume contribution region, while the traditional method utilizes them across the entire hypervolume region. For this reason, the approximation accuracy of the new method could be much higher than the traditional method when the same number of direction vectors are used in each method.

4 Numerical studies

4.1 Experiment settings

Solution sets generation. In our experiments, we consider three types of Pareto front (PF) shapes: linear, convex and concave. The linear PF is expressed as: $f_1 + f_2 + ... + f_m = 1$ and $f_i \geq 0$ for $i = 1, ..., m$. The concave PF is expressed as: $f_1^2 + f_2^2 + ... + f_m^2 = 1$ and $f_i \geq 0$ for $i = 1, ..., m$. The convex PF is expressed as: $(f_1 - 1)^2 + (f_2 - 1)^2 + ... + (f_m - 1)^2 = 1$ and $0 \leq f_i \leq 1$ for $i = 1, ..., m$.

For the two-dimensional case (i.e., $m = 2$), 50 solutions are randomly sampled from each PF to form three solution sets with different PF shapes. This sampling procedure is repeated until 1000 solution sets are generated for each PF shape. For the three-dimensional case (i.e., $m = 3$), 100 solutions are sampled from each PF and 1000 solution sets are generated for each PF shape. The generated solution sets are available at `https://github.com/nixizi/R2-HVC`.

The maximization case is considered. The reference point $\mathbf{r}$ for the hypervolume and R2 calculation is set as the origin.

Compared methods. Three methods for the hypervolume contribution approximation are compared. The first method is the traditional method described in Section 3.1. The second method is the new method proposed in Section 3.2. The third method is a simple method proposed in [7]. This method can be seen as a special version of the traditional method and the new method where only a single line segment connecting the reference point and a solution is used in this method for the hypervolume contribution approximation of the corresponding solution. More detailed explanations of this simple method can be found in [7].

For the traditional method, we use R_2^{HV} (Eq. (7)) as the R2 indicator and approximate the hypervolume contribution according to the R2 contribution (Eq. (8)). For the new method, we use R_2^{HVC} (Eq. (14)) for the approximation

and choose $\alpha = m$. The direction vectors used in the R2 indicators are generated by the simplex lattice design method[1].

In order to investigate the effect of the number of direction vectors on the performances of the three methods, we choose $\binom{H+1}{1}$ vectors where $H = 1, ..., 199$ in the two-dimensional case and $\binom{H+2}{2}$ vectors where $H = 1, ..., 50$ in the three-dimensional case[2].

4.2 Performance metrics

Two performance metrics are proposed to evaluate the performance of different methods for the hypervolume contribution approximation.

The first metric is the consistency rate in the order of the solution pairs in the solution set between their true hypervolume contributions and their hypervolume contributions approximated by different methods. Given a solution set A, there are a total number of $\binom{|A|}{2}$ solution pairs. For two solutions $\mathbf{s}_1$ and $\mathbf{s}_2$ from A, if the orders of their true hypervolume contributions and their approximated hypervolume contributions are the same, then the solution pair $(\mathbf{s}_1, \mathbf{s}_2)$ is called a consistent pair. The consistency rate of a solution set A is the ratio of the total number of the consistent pairs to $\binom{|A|}{2}$.

The second metric is the correct identification rate of the worst solution with the smallest hypervolume contribution in each solution set over all solution sets. For a solution set, if the solution with the smallest hypervolume contribution approximation identified by the method also has the smallest true hypervolume contribution, then we call this as a correct identification for this solution set. The correct identification rate is the ratio of the total number of the correct identifications to the total number of the solution sets.

For each type of solution sets (e.g., two-dimensional solution sets with the linear PF shape), there are a total number of 1000 solution sets. First the consistency rate for each solution set is calculated and then the average over the 1000 solution sets is obtained. The correct identification rate is determined by the proportion of the correct identification solution sets in the 1000 solution sets.

4.3 Results analysis

The results of the two performance metrics are shown in Fig. 6 and Fig. 7 respectively. From the figures we can obviously observe that the new method is superior to the other two methods in both of the performance metrics.

For the consistency rate (see Fig. 6), the new method can achieve a high consistency rate even when the number of vectors is small. The traditional method achieves a very low consistency rate when the number of vectors is small and gradually increases the consistency rate as the number of vectors increases. When

[1] First we use the simplex lattice design method to generate a set of weight vectors, then for each weight vector $\mathbf{w}$, the corresponding direction vector is $\lambda = \mathbf{w}/\|\mathbf{w}\|_2$.

[2] For the simplex lattice design method, the number of the vectors is determined by $\binom{H+m-1}{m-1}$ where m is the number of objectives and H is a positive integer.

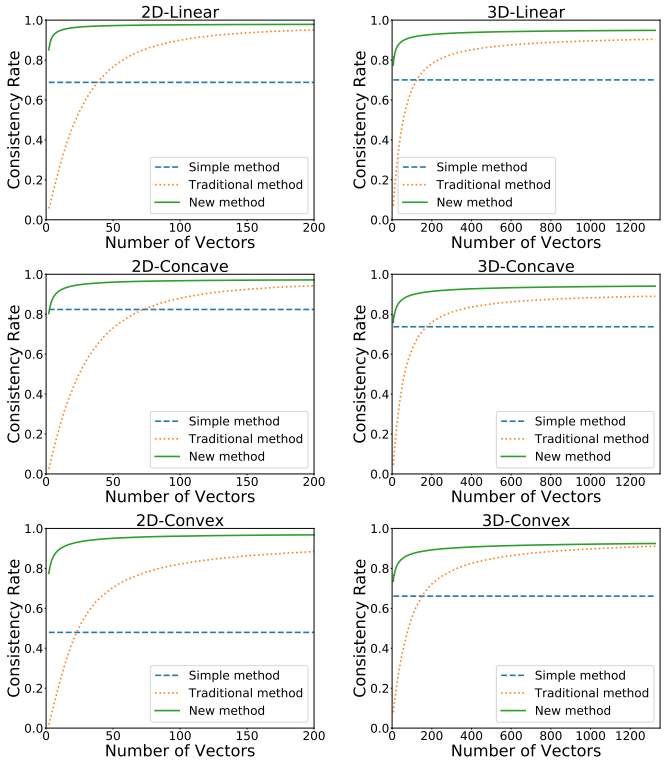


Fig. 6. Consistency rate on the two-dimension and three-dimension solution sets.

the number of vectors is large, the traditional method can achieve a high consistency rate but still worse than the new method. The simple method is a constant line because it always use only a single vector. This method can achieve a medium consistency rate compared with the other two methods.

For the correct identification rate (see Fig. 7), similar observations can be obtained. The new method achieves the best correct identification rate among the three methods. The traditional method shows a poor performance where the correct identification rate is 0 with a wide range of the number of vectors. The simple method performs better than the traditional method in most cases, but its performance is much lower than the new method.

With respect to the computation time of the three methods, the new method and the traditional method are almost the same with the same number of the direction vectors. The computation time of each method is proportional to the number of the direction vectors. For this reason, the simple method with only a single direction vector is the fastest.

In summary, the new method shows its clear advantage over the other two methods, where the new method is able to achieve a high approximation performance with only a small number of direction vectors.

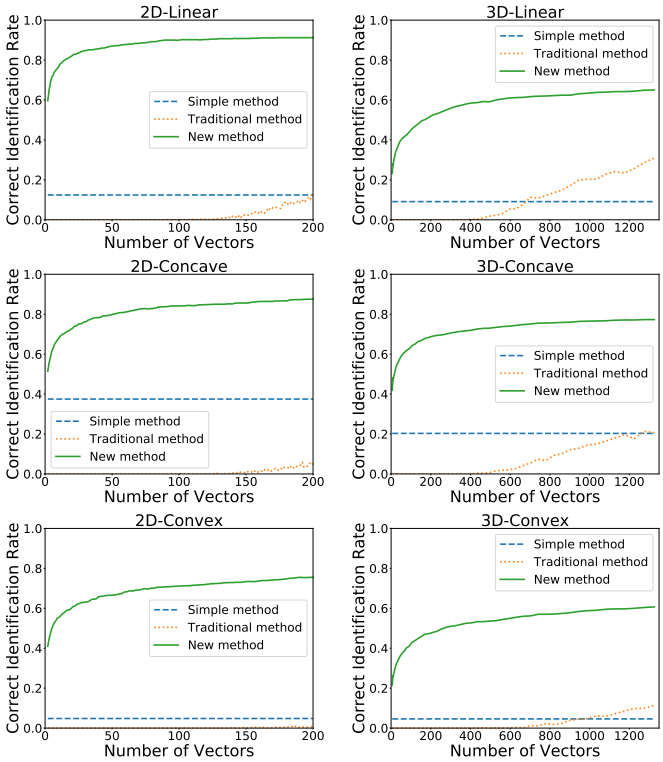


Fig. 7. Correct identification rate on the two-dimension and three-dimension solution sets.

5 Conclusions

In this paper, a new method for the hypervolume contribution approximation was proposed. The experimental results showed the overwhelming superiority of the new method over the other two methods for the hypervolume contribution approximation, where the new method was able to achieve a high approximation quality with only a small number of direction vectors. The proposed new method will bring opportunities for the development of new indicator-based EMOAs. One future research direction is to develop such an indicator-based EMOA and compare it with the hypervolume-based EMOAs [3,2] and other R2 indicator-based EMOAs [11,14,5,4]. Another future research direction is to investigate the approximation performance of the new method when a different direction vector generation method [8,9,13] is employed.

Acknowledgments. This work was supported by the Science and Technology Innovation Committee Foundation of Shenzhen (Grant No. ZDSYS201703031748284).

References

1. Bader, J., Deb, K., Zitzler, E.: Faster hypervolume-based search using monte carlo sampling. In: Multiple Criteria Decision Making for Sustainable Energy and Transportation Systems, pp. 313–326. Springer (2010)
2. Bader, J., Zitzler, E.: Hype: An algorithm for fast hypervolume-based many-objective optimization. Evolutionary computation 19(1), 45–76 (2011)
3. Beume, N., Naujoks, B., Emmerich, M.: Sms-emoa: Multiobjective selection based on dominated hypervolume. European Journal of Operational Research 181(3), 1653–1669 (2007)
4. Brockhoff, D., Wagner, T., Trautmann, H.: R2 indicator-based multiobjective search. Evolutionary Computation 23(3), 369–395 (2015)
5. Gómez, R.H., Coello, C.A.C.: Mombi: A new metaheuristic for many-objective optimization based on the r2 indicator. In: Evolutionary Computation (CEC), 2013 IEEE Congress on. pp. 2488–2495. IEEE (2013)
6. Ishibuchi, H., Tsukamoto, N., Sakane, Y., Nojima, Y.: Hypervolume approximation using achievement scalarizing functions for evolutionary many-objective optimization. In: Evolutionary Computation, 2009. CEC'09. IEEE Congress on. pp. 530–537. IEEE (2009)
7. Ishibuchi, H., Tsukamoto, N., Sakane, Y., Nojima, Y.: Indicator-based evolutionary algorithm with hypervolume approximation by achievement scalarizing functions. In: Proceedings of the 12th annual conference on Genetic and evolutionary computation. pp. 527–534. ACM (2010)
8. Li, K., Deb, K., Zhang, Q., Kwong, S.: An evolutionary many-objective optimization algorithm based on dominance and decomposition. IEEE Transactions on Evolutionary Computation 19(5), 694–716 (2015)
9. Ma, X., Qi, Y., Li, L., Liu, F., Jiao, L., Wu, J.: Moea/d with uniform decomposition measurement for many-objective problems. Soft Computing 18(12), 2541–2564 (2014)
10. Ma, X., Zhang, Q., Yang, J., Zhu, Z.: On tchebycheff decomposition approaches for multi-objective evolutionary optimization. IEEE Transactions on Evolutionary Computation (2017)
11. Phan, D.H., Suzuki, J.: R2-ibea: R2 indicator based evolutionary algorithm for multiobjective optimization. In: Evolutionary Computation (CEC), 2013 IEEE Congress on. pp. 1836–1845. IEEE (2013)
12. Shang, K., Ishibuchi, H., Zhang, M.L., Liu, Y.: A new r2 indicator for better hypervolume approximation. In: Proceedings of the Genetic and Evolutionary Computation Conference 2018. ACM (accepted)
13. Tan, Y.Y., Jiao, Y.C., Li, H., Wang, X.K.: Moea/d+ uniform design: A new version of moea/d for optimization problems with many objectives. Computers & Operations Research 40(6), 1648–1660 (2013)
14. Trautmann, H., Wagner, T., Brockhoff, D.: R2-emoa: Focused multiobjective search using r2-indicator-based selection. In: International Conference on Learning and Intelligent Optimization. pp. 70–74. Springer (2013)
15. Zitzler, E., Thiele, L.: Multiobjective optimization using evolutionary algorithms - a comparative case study. In: international conference on parallel problem solving from nature. pp. 292–301. Springer (1998)